Noname manuscript No.
(will be inserted by the editor)

Primordial gravitational waves and curvature perturbations induced energy density perturbation

Zhe Chang[1,2], **Yu-Ting Kuang**[a,1,2], **Xukun Zhang**[1,2], **Jing-Zhi Zhou**[1,2]

[1]Institute of High Energy Physics, Chinese Academy of Sciences, 100049 Beijing, China
[2]University of Chinese Academy of Sciences, Beijing 100049, China

Received: date / Accepted: date

Abstract We study the second order scalar and density perturbations generated by the Gaussian curvature perturbations and primordial gravitational waves in the radiation-dominated era. After presenting all the possible second-order source terms, we obtain the explicit expressions of the kernel functions and the power spectra of the second order scalar perturbations. It shows that the primordial gravitational waves might affect the second order energy density perturbation $\delta^{(2)} = \delta\rho^{(2)}/\rho^{(0)}$ significantly. The effects of the primordial gravitational waves are studied in terms of different kinds of primordial power spectra.

Keywords primordial gravitational waves · cosmological perturbation theory · primordial power spectra

arXiv:2211.11948v3 [astro-ph.CO] 29 Jan 2024

1 Introduction

The cosmological perturbations which are originated from the quantum fluctuations during inflation will inevitably induce higher order perturbations. These induced higher order perturbations can also affect the evolutions of the universe [1].

The cosmological perturbations can be decomposed as scalar, vector, and tensor perturbations on account of the $SO(3)$ symmetry of the Friedmann-Robertson-Walker (FRW) spacetime [2–4]. Recently, the higher order perturbations induced by the primordial perturbations have been attracting a lot of interests because of their rich phenomenology [5]. For tensor perturbation, the higher order induced tensor perturbations are known as induced gravitational waves (GWs) [6–31]. For higher order induced scalar perturbations [32–34], the higher order energy density perturbation $\delta^{(n)} = \rho^{(n)}/\rho^{(0)}$ can be calculated in terms of these scalar perturbations. And $\delta^{(n)}$ can affect the primordial black hole (PBH) formation [35, 36], and the large-scale structure (LSS) of the Universe [37, 38]. The higher order induced vector perturbations can also affect many cosmological observations [5, 39–48], such as redshift-space distortions [42] and weak lensing [45–47].

The source terms of high order induced perturbations originate from the primordial perturbations generated during the inflation. Since vector perturbations decay as $1/a^2$ [39], we typically

[a]e-mail: kuangyt@ihep.ac.cn

neglect the primordial vector perturbations. On large scales ($\geq 1Mpc$), the amplitude of the primordial scalar perturbation A_ζ is constrained by observations of the Cosmic Microwave Background (CMB) and large-scale structures to be about $A_\zeta \simeq 2^{-9}$. For the primordial tensor perturbation on large scales ($\geq 1Mpc$), the tensor-to-scalar ratio $r = A_h/A_\zeta$ is constrained to be less than 0.06 [49], where A_h is the amplitude of primordial tensor perturbation. Therefore, when studying higher order induced perturbations on large scales ($\geq 1Mpc$), primordial tensor perturbation can be neglected compared to primordial scalar perturbation.

On small scales ($\leq 1Mpc$), the constraints of primordial scalar and tensor perturbations are significantly weaker than those on large scales [50]. Over the past few years, the primordial scalar perturbation with large amplitude on small scales have been attracting a lot of interest. It is closely related to primordial black holes and scalar induced GWs [51–56]. For the primordial tensor perturbation on small scales, its amplitude could also be much larger than it is on the large scales. The large primordial tensor perturbation on small scales can be realized by many models of early universe, such as G^2-inflation [57], spectator field [58], and so on [35]. Recently, the power spectra of second order tensor perturbation induced by primordial scalar and tensor perturbations with large amplitudes were studied in Ref. [17, 59–61]. They considered the log-normal primordial scalar and tensor power spectra on small scales and found that the primordial tensor perturbation has a very important effect on the second order induced tensor perturbation.

The second order induced scalar and energy density perturbations have been studied for many years [32–38, 62]. However, a complete study of the second order induced scalar perturbations has not been presented. The importance of the scalar-tensor coupling source terms $\mathcal{S}_2 \sim \phi h$ has been neglected in previous studies. In this paper, we consider the second order energy density perturbation induced by primordial curvature and tensor perturbations during RD era systematically. The second order scalar perturbations can be generated by the scalar-scalar, scalar-tensor, and tensor-tensor coupling source terms: $\mathcal{S}_1 \sim \phi\phi$, $\mathcal{S}_2 \sim \phi h$, and $\mathcal{S}_3 \sim hh$. The second order energy density perturbation $\mathcal{P}_\delta^{(2)}$ can be calculated in terms of these second order induced scalar perturbations.The explicit expressions of second order scalar and energy density perturbations are presented in this work.

This paper is organized as follows. In Sec. 2, the second order scalar perturbations are studied. The explicit expressions of the second order power spectra are presented. In Sec. 3, we investigate the second order power spectrum in terms of the monochromatic primordial power spectra. The $\mathcal{P}_\delta^{(2)}$ induced by log-normal primordial power spectra are studied in Sec. 4. The conclusions and discussions are summarized in Sec. 5.

2 Second order scalar perturbations

In this section, we study the equations of motion and the kernel functions of the second order scalar perturbations induced by primordial curvature and tensor perturbations in the RD era.

2.1 Equation of motion

The perturbed metric in the flat FRW spacetime with Newtonian gauge is given by

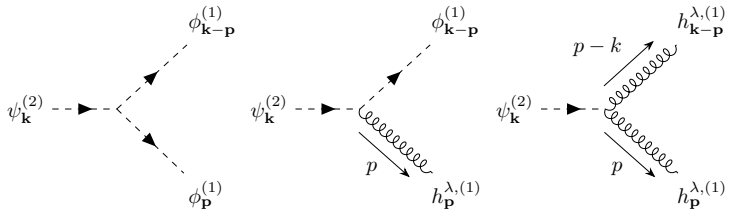
$$\mathrm{d}s^2 = a^2\left[-\left(1+2\phi^{(1)}+\phi^{(2)}\right)\mathrm{d}\eta^2+\left(\left(1-2\psi^{(1)}-\psi^{(2)}\right)\delta_{ij}+h_{ij}^{(1)}\right)\mathrm{d}x^i\mathrm{d}x^j\right], \tag{1}$$

where $\phi^{(n)}$ and $\psi^{(n)}(n=1,2)$ are first order and second order scalar perturbations, $h_{ij}^{(1)}$ is the first order tensor perturbation. Here, we neglect the first order vector perturbation since the vector modes decay as $1/a^2$ after they leaving the Hubble horizon during inflation. We use `xPand` package to study the perturbations of Einstein equation, `xPand` package can help us to obtain and simplify the equations of motion of cosmological perturbations [63]. The equations of motion of second order scalar perturbations are given by

$$\Psi^{(2)}-\Phi^{(2)} = -2\Delta^{-1}\left(\partial^i\Delta^{-1}\partial^j-\frac{1}{2}\mathcal{T}^{ij}\right)\mathcal{S}_{ij}\left(\mathbf{x},\eta\right), \tag{2}$$

$$\partial_\eta^2\Psi^{(2)}+3\mathcal{H}\partial_\eta\Psi^{(2)}-\frac{5}{6}\Delta\Psi^{(2)}+\mathcal{H}\partial_\eta\Phi^{(2)}+\frac{1}{2}\Delta\Phi^{(2)} = -\frac{1}{2}\mathcal{T}^{ij}\mathcal{S}_{ij}\left(\mathbf{x},\eta\right), \tag{3}$$

where $\mathcal{T}^{ij}=\delta^{ij}-\partial^i\Delta^{-1}\partial^j$ is the transverse operator. During the RD era, the conformal Hubble parameter can be expressed as $\mathcal{H}=1/\eta$. For convenience, we use the symbols $\phi^{(1)}\equiv\phi$ and $h_{ij}^{(1)}\equiv h_{ij}$. As shown in Fig. 1, the source term $\mathcal{S}_{ij}\left(\mathbf{x},\eta\right)$ is composed of three parts $\mathcal{S}_{ij}\left(\mathbf{x},\eta\right)=\mathcal{S}_{ij,1}+\mathcal{S}_{ij,2}+\mathcal{S}_{ij,3}$. The explicit expressions of the source terms are given in Appendix A. Substituting



(a) $\mathcal{S}_{ij,1}\sim\phi^{(1)}\phi^{(1)}$ (b) $\mathcal{S}_{ij,2}\sim\phi^{(1)}h^{\lambda,(1)}$ (c) $\mathcal{S}_{ij,3}\sim h^{\lambda,(1)}h^{\lambda,(1)}$

Fig. 1: The source terms $\mathcal{S}_{ij,1}$ is composed of the first order scalar perturbation, the source terms $\mathcal{S}_{ij,2}$ is composed of the product of the first order scalar perturbation and the first order tensor perturbation, and the source terms $\mathcal{S}_{ij,3}$ is composed of the first order tensor perturbation.

Eq. (2) into Eq. (3), we obtain the equation of motion of second order scalar perturbation $\Psi^{(2)}$ in

the RD era

$$\begin{aligned}
&\partial_\eta^2\Psi^{(2)}+\frac{4}{\eta}\partial_\eta\Psi^{(2)}-\frac{1}{3}\Delta\Psi^{(2)}\\
&=-\frac{1}{2}\mathcal{T}^{ij}S_{ij}-2\Delta^{-1}\left(\partial^j\Delta^{-1}\partial^i-\frac{1}{2}\mathcal{T}^{ij}\right)\left(\frac{1}{2}\Delta+\frac{1}{\eta}\partial_\eta\right)\mathcal{S}_{ij}\left(\mathbf{x},\eta\right)\\
&=\left(-\frac{1}{2}\mathcal{T}^{ij}-\left(\partial^j\Delta^{-1}\partial^i-\frac{1}{2}\mathcal{T}^{ij}\right)-2\Delta^{-1}\left(\partial^j\Delta^{-1}\partial^i-\frac{1}{2}\mathcal{T}^{ij}\right)\frac{1}{\eta}\partial_\eta\right)S_{ij}\left(\mathbf{x},\eta\right)\\
&=-\left(\partial^j\Delta^{-1}\partial^i+2\Delta^{-1}\left(\partial^j\Delta^{-1}\partial^i-\frac{1}{2}\mathcal{T}^{ij}\right)\frac{1}{\eta}\partial_\eta\right)\sum_{a=1}^{3}\mathcal{S}_{ij,a}\left(\mathbf{x},\eta\right)\ .
\end{aligned}\tag{4}$$

2.2 Kernel functions

In order to solve the equation of motion of second order scalar perturbation, we rewrite Eq. (4) in momentum space as

$$\Psi^{(2)''}\left(\mathbf{k},\eta\right)+\frac{4}{\eta}\Psi^{(2)'}\left(\mathbf{k},\eta\right)+\frac{k^2}{3}\Psi^{(2)}\left(\mathbf{k},\eta\right)=\sum_{a=1}^{3}\mathcal{S}_a\left(\mathbf{k},\eta\right)\ ,\tag{5}$$

where

$$\mathcal{S}_a\left(\mathbf{k},\eta\right)=\mathcal{D}_\psi^{ij}\mathcal{S}_{ij,a}\left(\mathbf{k},\eta\right)\ ,\quad \mathcal{D}_\psi^{ij}=-\left(\frac{k^ik^j}{k^2}-\left(\frac{3k^ik^j}{k^4}-\frac{\delta^{ij}}{k^2}\right)\frac{k^2}{x}\partial_x\right)\ .\tag{6}$$

Here, we have defined $x\equiv k\eta$. The explicit expressions of $\mathcal{S}_{ij,a}\left(\mathbf{k},\eta\right)(a=1,2,3)$ are given in Appendix A. Substituting Eqs. (A.4)–(A.6) into Eq. (6), we obtain the expressions of $\mathcal{S}_a\left(\mathbf{k},\eta\right)$

$$\mathcal{S}_1=\mathcal{D}_\psi^{ij}\mathcal{S}_{ij,1}=\int\frac{d^3p}{(2\pi)^{3/2}}k^2f_1\left(u,v,x\right)\frac{4}{9}\zeta_{\mathbf{k}-\mathbf{p}}\zeta_{\mathbf{p}}\ ,\tag{7}$$

$$\mathcal{S}_2=\mathcal{D}_\psi^{ij}\mathcal{S}_{ij,2}=\int\frac{d^3p}{(2\pi)^{3/2}}k^2f_2^{\lambda_1}\left(u,v,x\right)\frac{2}{3}\zeta_{\mathbf{k}-\mathbf{p}}\mathbf{h}_{\mathbf{p}}^{\lambda_1}\ ,\tag{8}$$

$$\mathcal{S}_3=\mathcal{D}_\psi^{ij}\mathcal{S}_{ij,3}=\int\frac{d^3p}{(2\pi)^{3/2}}k^2f_3^{\lambda_1\lambda_2}\left(u,v,x\right)\mathbf{h}_{\mathbf{k}-\mathbf{p}}^{\lambda_1}\mathbf{h}_{\mathbf{p}}^{\lambda_2}\ ,\tag{9}$$

where λ_1 and λ_2 are the polarization indices, the spatial indices of $\mathcal{S}_{ij,a}(a=1,2,3)$ are contracted. Substituting Eqs. (7)–(9) into Eq. (5), we solve the Eq. (5) by using the Green's function method

$$\Psi^{(2)}=\sum_{a=1}^{3}\Psi_a^{(2)}\ ,\ (a=,1,2,3)\ ,\tag{10}$$

where

$$\Psi_1^{(2)}=\int\frac{d^3p}{(2\pi)^{3/2}}I_1\left(u,v,x\right)\frac{4}{9}\zeta_{\mathbf{k}-\mathbf{p}}\zeta_{\mathbf{p}}\ ,\tag{11}$$

$$\Psi_2^{(2)}=\int\frac{d^3p}{(2\pi)^{3/2}}I_2^{\lambda_1}\left(u,v,x\right)\frac{2}{3}\zeta_{\mathbf{k}-\mathbf{p}}\mathbf{h}_{\mathbf{p}}^{\lambda_1}\ ,\tag{12}$$

$$\Psi_3^{(2)}=\int\frac{d^3p}{(2\pi)^{3/2}}I_3^{\lambda_1\lambda_2}\left(u,v,x\right)\mathbf{h}_{\mathbf{k}-\mathbf{p}}^{\lambda_1}\mathbf{h}_{\mathbf{p}}^{\lambda_2}\ .\tag{13}$$

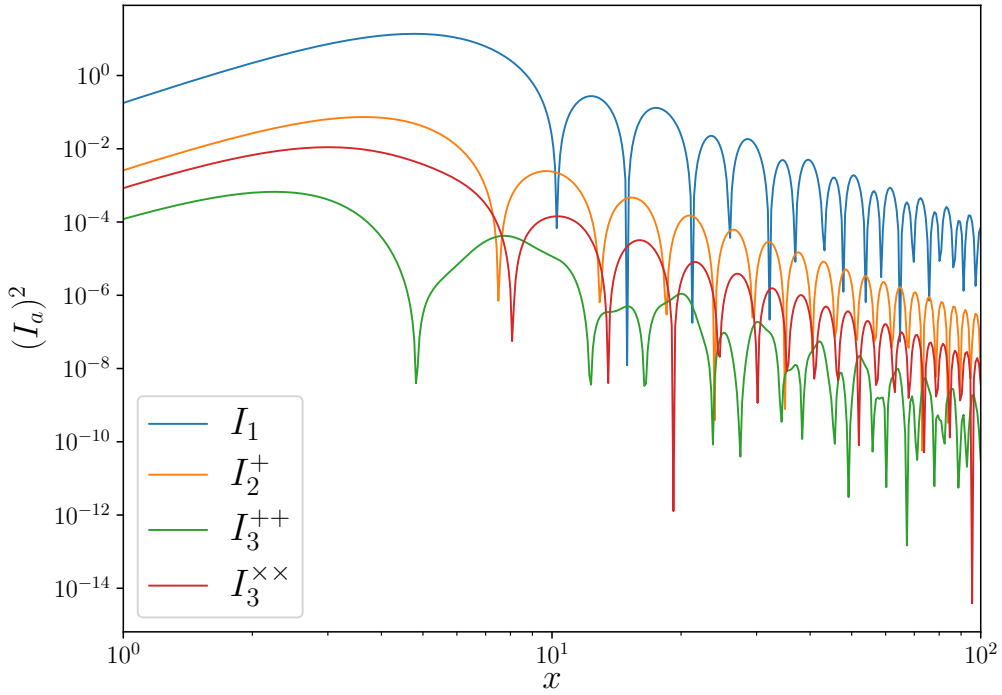


Fig. 2: The kernel functions I_i $(i = 1, 2, 3)$ in Eq. (14). We have set $u = v = 1$.

In Eqs. (11)–(13), the kernel functions $I_a(u, v, x)(a = 1, 2, 3)$ are defined as

$$
\begin{aligned}
I_1 &= \int_0^x \mathrm{d}\bar{x} \left(\frac{\bar{x}}{x}\right)^2 \left\{-\frac{x\bar{x}}{\sqrt{3}}\left[j_1(x/\sqrt{3})y_1(\bar{x}/\sqrt{3}) - j_1(\bar{x}/\sqrt{3})y_1(x/\sqrt{3})\right]\right\} f_1(u, v, \bar{x}) \ , \\
I_2^{\lambda_1} &= \int_0^x \mathrm{d}\bar{x} \left(\frac{\bar{x}}{x}\right)^2 \left\{-\frac{x\bar{x}}{\sqrt{3}}\left[j_1(x/\sqrt{3})y_1(\bar{x}/\sqrt{3}) - j_1(\bar{x}/\sqrt{3})y_1(x/\sqrt{3})\right]\right\} f_2^{\lambda_1}(u, v, \bar{x}) \ , \\
I_3^{\lambda_1,\lambda_2} &= \int_0^x \mathrm{d}\bar{x} \left(\frac{\bar{x}}{x}\right)^2 \left\{-\frac{x\bar{x}}{\sqrt{3}}\left[j_1(x/\sqrt{3})y_1(\bar{x}/\sqrt{3}) - j_1(\bar{x}/\sqrt{3})y_1(x/\sqrt{3})\right]\right\} f_3^{\lambda_1,\lambda_2}(u, v, \bar{x}) \ .
\end{aligned}
\tag{14}
$$

In the end of this section, we calculate the kernel functions in Eq. (14). We present these three kinds of kernel functions $(I_a(u = 1, v = 1, x))^2(a = 1, 2, 3)$ as functions of $x = k\eta$ in Fig. 2. As shown in Fig. 2, the kernel function I_1 is much larger than other kernel functions.

2.3 Initial second order perturbation

As we mentioned in Ref. [2, 32], the contributions from the initial second-order perturbation also need to considered. More precisely, the second order scalar perturbations are composed of two parts, the second order scalar perturbations induced by the primordial perturbations and the initial second-order perturbation. The second-order curvature perturbation in the Newtonian gauge is given by [2]

$$
-\zeta^{(2)} = \Psi^{(2)} + \frac{\mathcal{H}}{\rho^{(0)\prime}}\left[\delta\rho^{(2)} - \frac{\delta\rho^{(1)\prime}}{\rho^{(0)\prime}}\delta\rho^{(1)}\right] - \frac{1}{4}\chi^k_{\delta\rho k} + \frac{1}{4}\Delta^{-2}\partial^i\partial^j\chi_{ij\delta\rho} \ , \tag{15}
$$

where

$$\begin{aligned}\chi_{ij\delta\rho} \equiv & -2\frac{\mathcal{H}}{\rho^{(0)\prime}}\left[2\mathcal{H}\left(\frac{\delta\rho^{(1)2}}{\rho^{(0)\prime}}\right)-\frac{\delta\rho^{(1)\prime}}{\rho^{(0)\prime}}\delta\rho^{(1)}\right]\delta_{ij}-\frac{2}{\rho^{(0)\prime 2}}\partial_i\delta\rho^{(1)}\partial_j\delta\rho^{(1)} \\ & +4\left[-\frac{\delta\rho^{(1)}}{\rho^{(0)\prime}}\left[\left(-\Psi^{(1)\prime}\delta_{ij}+\frac{1}{2}h_{ij}^{(1)\prime}\right)+2\mathcal{H}\left(-\Psi^{(1)}\delta_{ij}+\frac{1}{2}h_{ij}^{(1)}\right)\right]\right] ,\end{aligned} \tag{16}$$

$$\begin{aligned}\chi^{k}_{\delta\rho k} \equiv & -6\frac{\mathcal{H}}{\rho^{(0)\prime}}\left[2\mathcal{H}\left(\frac{\delta\rho^{(1)2}}{\rho^{(0)\prime}}\right)-\frac{\delta\rho^{(1)\prime}}{\rho^{(0)\prime}}\delta\rho^{(1)}\right]-\frac{2}{\rho^{(0)\prime 2}}\partial^k\delta\rho^{(1)}\partial_k\delta\rho^{(1)} \\ & +4\left[-\frac{\delta\rho^{(1)}}{\rho^{(0)\prime}}\left[\left(-3\Psi^{(1)\prime}+\frac{1}{2}h_{k}^{(1)k\prime}\right)+2\mathcal{H}\left(-3\Psi^{(1)}+\frac{1}{2}h_{k}^{(1)k}\right)\right]\right] .\end{aligned} \tag{17}$$

In the superhorizon limit ($k\eta \ll 1$), the second-order curvature perturbation can be approximated as

$$\begin{aligned}\zeta^{(2)}(k,\eta) \simeq & \left\{-\Psi^{(2)}(k,\eta)+\frac{1}{4}\delta^{(2)}-\frac{1}{8}\delta^{(1)2}-\delta^{(1)}\Psi^{(1)}\right. \\ & \left.+\frac{\delta^{(1)}h_k^{(1)k}}{4}-\frac{\delta^{(1)}\nabla^{-2}\partial_i\partial_j h^{(1)ij}}{4}\right\}T_\Psi(k\eta) ,\end{aligned} \tag{18}$$

where

$$\delta^{(1)}=\frac{\delta\rho^{(1)}}{\rho^{(0)}}=\frac{-6\mathcal{H}\left(\mathcal{H}\phi^{(1)}+\psi^{(1)\prime}\right)+2\triangle\psi^{(1)}}{3\mathcal{H}^2}\simeq -2\phi^{(1)}=-\frac{4}{3}\zeta^{(1)} . \tag{19}$$

We assume the local type non-Gaussianity here, which is parametrized as $\zeta^{(2)}=2a_{\rm NL}\left(\zeta^{(1)}\right)^2$ in the superhorizon limit, and $a_{\rm NL}=1$ for Gaussian perturbation [64–66]. Substituting the condition of the local type non-Gaussianity into Eq. (18), we obtain the contributions from the initial second-order perturbation

$$\begin{aligned}\Psi^{(2)}_{\rm in}(\mathbf{k}) = & \frac{1}{3}\left(\frac{3k^ik^j}{k^4}-\frac{\delta^{ij}}{k^2}\right)\mathcal{S}_{ij}+\int\frac{d^3p}{(2\pi)^{3/2}}\left(\left(-\frac{4}{3}a_{\rm NL}+\frac{28}{27}\right)\zeta_{\mathbf{k}-\mathbf{p}}\zeta_{\mathbf{p}}\right. \\ & \left.-\frac{2}{9}\varepsilon_i^{\lambda,i}(\mathbf{p})\,\zeta_{\mathbf{k}-\mathbf{p}}\mathbf{h}^\lambda_{\mathbf{p}}+\frac{2}{9}\frac{p^ip^j}{p^2}\varepsilon^\lambda_{ij}(\mathbf{p})\,\zeta_{\mathbf{k}-\mathbf{p}}\mathbf{h}^\lambda_{\mathbf{p}}\right) .\end{aligned} \tag{20}$$

After considering the effects of the initial second-order perturbation, the second order scalar perturbation $\Psi^{(2)}$ can be written as

$$\Psi^{(2)}(\mathbf{k})=\Psi^{(2)}_{\rm in}(\mathbf{k})+\sum_{a=1}^{3}\Psi^{(2)}_a\ ,\ (a=,1,2,3) . \tag{21}$$

We study the second order scalar and density perturbations generated by the Gaussian curvature and tensor perturbations. Therefore, we set $a_{\rm NL}=1$ in this paper.

2.4 Power spectra

In this section, the power spectra of second order scalar and density perturbations are investigated. We assume that the two-point function $\langle\zeta_{\mathbf{k}_1}\mathbf{h}^\lambda_{\mathbf{k}_2}\rangle$=0 for arbitrary $\mathbf{k}_1$ and $\mathbf{k}_2$ [17]. Therefore, we only need to consider three kinds of four-point functions. The explicit expressions of these four-point functions are given in Appendix C. The power spectra of second order scalar perturbation is defined as

$$\langle\Psi^{(2)}(\mathbf{k})\,\Psi^{(2)}\left(\mathbf{k}'\right)\rangle=\delta\left(\mathbf{k}+\mathbf{k}'\right)\frac{2\pi^2}{k^3}\mathcal{P}^{(2)}_\psi . \tag{22}$$

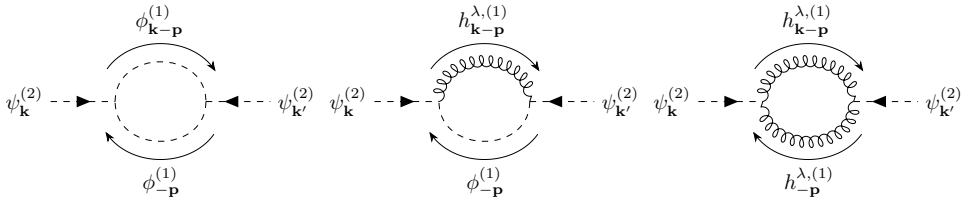
Substituting Eqs. (11)–(13) into Eq. (22), we obtain

$$\langle \Psi^{(2)}\left(\mathbf{k}\right)\Psi^{(2)}\left(\mathbf{k}'\right)\rangle = \sum_{i=1}^{3}\langle \Psi_i^{(2)}\left(\mathbf{k}\right)\Psi_i^{(2)}\left(\mathbf{k}'\right)\rangle \ , \tag{23}$$

where

$$\begin{aligned}
\langle \Psi_1^{(2)}\left(\mathbf{k}\right)\Psi_1^{(2)}\left(\mathbf{k}'\right)\rangle =& \int \frac{d^3p}{(2\pi)^{3/2}}\frac{d^3p'}{(2\pi)^{3/2}} I_1\left(|\mathbf{k}-\mathbf{p}|,p,\eta\right) I_1\left(|\mathbf{k}'-\mathbf{p}'|,p',\eta\right) \\
&\times \frac{16}{81}\langle \zeta_{\mathbf{k}-\mathbf{p}}\zeta_{\mathbf{p}}\zeta_{\mathbf{k}'-\mathbf{p}'}\zeta_{\mathbf{p}'}\rangle \ , \qquad (24)\\
\langle \Psi_2^{(2)}\left(\mathbf{k}\right)\Psi_2^{(2)}\left(\mathbf{k}'\right)\rangle =& \int \frac{d^3p}{(2\pi)^{3/2}}\frac{d^3p'}{(2\pi)^{3/2}} I_2^{\lambda_1}\left(|\mathbf{k}-\mathbf{p}|,p,\eta\right) I_2^{\lambda_1'}\left(|\mathbf{k}'-\mathbf{p}'|,p',\eta\right) \\
&\times \frac{4}{9}\langle \zeta_{\mathbf{k}-\mathbf{p}}\mathbf{h}_{\mathbf{p}}^{\lambda_1}\zeta_{\mathbf{k}'-\mathbf{p}'}\mathbf{h}_{\mathbf{p}'}^{\lambda_1'}\rangle \ , \qquad (25)\\
\langle \Psi_3^{(2)}\left(\mathbf{k}\right)\Psi_3^{(2)}\left(\mathbf{k}'\right)\rangle =& \int \frac{d^3p}{(2\pi)^{3/2}}\frac{d^3p'}{(2\pi)^{3/2}} I_3^{\lambda_1\lambda_2}\left(|\mathbf{k}-\mathbf{p}|,p,\eta\right) I_3^{\lambda_1'\lambda_2'}\left(|\mathbf{k}'-\mathbf{p}'|,p',\eta\right) \\
&\times \langle \mathbf{h}_{\mathbf{k}-\mathbf{p}}^{\lambda_1}\mathbf{h}_{\mathbf{p}}^{\lambda_2}\mathbf{h}_{\mathbf{k}'-\mathbf{p}'}^{\lambda_1'}\mathbf{h}_{\mathbf{p}'}^{\lambda_2'}\rangle \ . \qquad (26)
\end{aligned}$$

The corresponding Feynman diagrams of these three kinds of two-point functions are given in Fig. 3 Substituting Eqs. (C.15)–(C.17) into Eqs. (24)–(26), we obtain the explicit expressions of the power



(a) $\mathcal{P}_1^{(2)} \sim \langle \Psi_1^{(2)}\left(\mathbf{k}\right)\Psi_1^{(2)}\left(\mathbf{k}'\right)\rangle$ (b) $\mathcal{P}_2^{(2)} \sim \langle \Psi_2^{(2)}\left(\mathbf{k}\right)\Psi_2^{(2)}\left(\mathbf{k}'\right)\rangle$ (c) $\mathcal{P}_3^{(2)} \sim \langle \Psi_3^{(2)}\left(\mathbf{k}\right)\Psi_3^{(2)}\left(\mathbf{k}'\right)\rangle$

Fig. 3: The Feynman diagrams of three kinds of two-point functions.

spectra

$$\mathcal{P}_\psi^{(2)} = \mathcal{P}_1^{(2)} + \mathcal{P}_2^{(2)} + \mathcal{P}_3^{(2)} \ , \tag{27}$$

where

$$\mathcal{P}_1^{(2)} = \frac{1}{2}\int_0^\infty dv \int_{|1-v|}^{|1+v|} \frac{du}{v^2u^2} I_1(u,v,x)\,\mathcal{P}_\zeta(uk)\mathcal{P}_\zeta(vk) \times \frac{16}{81}\left[I_1\left(|\mathbf{k}'-\mathbf{p}'|,p',\eta\right)\big|_{\mathbf{p}'=-\mathbf{p}} + I_1\left(|\mathbf{k}'-\mathbf{p}'|,p',\eta\right)\big|_{\mathbf{p}'=\mathbf{p}-\mathbf{k}}\right]\Big|_{\mathbf{k}'\to-\mathbf{k}}, \tag{28}$$

$$\mathcal{P}_2^{(2)} = \frac{1}{2}\int_0^\infty dv \int_{|1-v|}^{|1+v|} \frac{du}{v^2u^2} I_2^{\lambda_1}(u,v,x)\,\delta^{\lambda_1\lambda_1'}\mathcal{P}_\zeta(uk)\mathcal{P}_h(vk) \times \frac{4}{9} I_2^{\lambda_1'}\left(|\mathbf{k}'-\mathbf{p}'|,p',\eta\right)\big|_{\mathbf{p}'=-\mathbf{p},\ \mathbf{k}'=-\mathbf{k}}, \tag{29}$$

$$\mathcal{P}_3^{(2)} = \frac{1}{2}\int_0^\infty dv \int_{|1-v|}^{|1+v|} \frac{du}{v^2u^2} I_3^{\lambda_1\lambda_2}(u,v,x)\,\mathcal{P}_h(uk)\mathcal{P}_h(vk) \times \Big[\delta^{\lambda_1\lambda_1'}\delta^{\lambda_2\lambda_2'} I_3^{\lambda_1'\lambda_2'}\left(|\mathbf{k}'-\mathbf{p}'|,p',\eta\right)\big|_{\mathbf{p}'=-\mathbf{p}} + \delta^{\lambda_1\lambda_2'}\delta^{\lambda_2\lambda_1'} I_3^{\lambda_1'\lambda_2'}\left(|\mathbf{k}'-\mathbf{p}'|,p',\eta\right)\big|_{\mathbf{p}'=\mathbf{p}-\mathbf{k}}\Big]\Big|_{\mathbf{k}'=-\mathbf{k}}. \tag{30}$$

In Eqs. (28)–(30), the substitutions of $\mathbf{k}'$ and $\mathbf{p}'$ come from the three dimensional delta functions in the Wick's expansions of four-point functions. Since we have assumed the two-point function $\langle\zeta_{\mathbf{k}_1}\mathbf{h}^\lambda_{\mathbf{k}_2}\rangle$=0, three kinds of source terms in Eqs. (A.1)–(A.3) are decoupled. More precisely, the two-point functions $\langle\Psi_i^{(2)}(\mathbf{k})\,\Psi_j^{(2)}(\mathbf{k}')\rangle = 0$ if $i\neq j$. As shown in Eqs. (28)–(30), the power spectra of second order scalar perturbation are composed of three parts, which come from the source terms $\mathcal{S}_1\sim\phi\phi$, $\mathcal{S}_2\sim\phi h$, and $\mathcal{S}_3\sim hh$ respectively.

The energy density perturbation can be calculated as

$$\delta^{(2)} = \frac{\delta\rho^{(2)}}{\rho^{(0)}} = -\frac{1}{3\mathcal{H}^4}\left(\frac{1}{4}\mathcal{H}^2 h'_{ij}\left(h'^{ij}+8\mathcal{H}h^{ij}\right) + 6\mathcal{H}^4\left(-4\phi^2+\Phi^{(2)}\right) + 6\mathcal{H}^3\Psi^{(2)'} + 4\mathcal{H}\partial_i\phi'\partial^i\phi + 2\partial_i\phi'\partial^i\phi' + \mathcal{H}^2\left(-2\left(3\phi'^2+8\phi\Delta\phi+\Delta\Psi^{(2)}+2\partial_i\phi\partial^i\phi+\frac{1}{2}h^{ij}\left(-\partial_i\partial_j\phi+\Delta h_{ij}\right)\right) + \frac{1}{4}\left(2\partial_l h_{ij}-3\partial_j h_{il}\right)\partial^j h^{il}\right)\right). \tag{31}$$

The power spectrum of second order energy density perturbation $\mathcal{P}_\delta^{(2)}$ is defined by

$$\langle\delta^{(2)}(\mathbf{k})\,\delta^{(2)}(\mathbf{k}')\rangle = \delta\left(\mathbf{k}+\mathbf{k}'\right)\frac{2\pi^2}{k^3}\mathcal{P}_\delta^{(2)}, \tag{32}$$

where the energy density $\delta^{(2)}$ can be calculated in terms of Eq. (21) and Eq. (31).

3 Monochromatic primordial power spectra

As mentioned, the constraints of primordial curvature and tensor perturbations on small scales are significantly weaker than those on large scales, the tensor-to-scalar ratio r can be very large on small scales. Therefore, we start with a toy model of δ-peak. In this case, the primordial scalar and tensor perturbations are very large on small scalar. Since we consider the second order scalar and density perturbations generated by the Gaussian curvature and tensor perturbations, we have set $a_{\rm NL}=1$ in the Eq. (20).

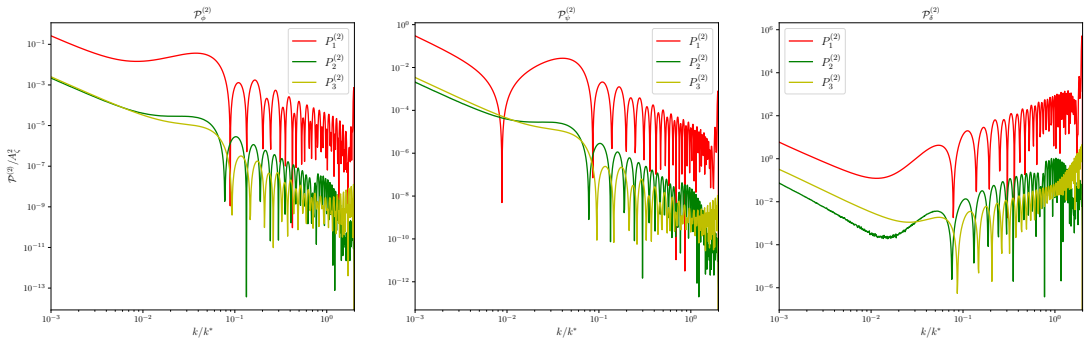


Fig. 4: The three kinds of power spectra $\mathcal{P}_a^{(2)}(a=1,2,3)$ for second order perturbations $\Phi^{(2)}$, $\Psi^{(2)}$, and $\delta^{(2)}$. The power spectra $\mathcal{P}_1^{(2)}$, $\mathcal{P}_2^{(2)}$, and $\mathcal{P}_3^{(2)}$ come from the source terms $\mathcal{S}_1 \sim \phi\phi$, $\mathcal{S}_2 \sim \phi h$, and $\mathcal{S}_3 \sim hh$ respectively. We have set the tensor-to-scalar ratio $r = A_h/A_\zeta = 1$, and $x_* = k_*\eta = 100$.

3.1 Monochromatic primordial power spectra with the same k_*

We consider the monochromatic primordial power spectra, namely

$$\mathcal{P}_\zeta = A_\zeta k_{\zeta *}\delta\left(k-k_{\zeta *}\right)\ ,\ \mathcal{P}_h = A_h k_{h*}\delta\left(k-k_{h*}\right)\ ,\ k_{\zeta *}=k_{h*}=k_*\ , \tag{33}$$

where k_* is the wavenumber at which the power spectrum has a δ-function peak. In Fig. 4, we plot the three kinds of power spectra for second order perturbations $\Phi^{(2)}$, $\Psi^{(2)}$, and $\delta^{(2)}$. Here, we use the symbols $\mathcal{P}_1^{(2)}$, $\mathcal{P}_2^{(2)}$, and $\mathcal{P}_3^{(2)}$ to represent the contributions of the source terms $\mathcal{S}_1 \sim \phi\phi$, $\mathcal{S}_2 \sim \phi h$ and $\mathcal{S}_3 \sim hh$ respectively. As shown in Fig. 4, for tensor-to-scalar ratio $r = A_h/A_\zeta = 1$, the second order perturbations sourced by $\mathcal{S}_1 \sim \phi\phi$ dominate the total power spectra of $\Phi^{(2)}$, $\Psi^{(2)}$, and $\delta^{(2)}$.

In order to study the effects of the large tensor-to-scalar ratio $r = A_h/A_\zeta$ on small scales, we calculate the total power spectra of $\Phi^{(2)}$, $\Psi^{(2)}$, and $\delta^{(2)}$ for different $r = A_h/A_\zeta$. In Fig. 5, the total power spectra of second order scalar perturbations for different r are presented. For tensor-to-scalar ratio $r \ll 1$, the effects of primordial tensor perturbation become negligible, the total power spectra $\mathcal{P}_\phi^{(2)}$, $\mathcal{P}_\psi^{(2)}$, and $\mathcal{P}_\delta^{(2)}$ reduce to the results in Ref. [32]. For $r \gg 1$ on small scales, the effects of the primordial tensor perturbation become obvious, the total power spectra reduce to the results in Ref. [35, 37, 38].

3.2 Monochromatic primordial power spectra with different k_*

The monochromatic primordial power spectra with different k_* can be written as

$$\mathcal{P}_\zeta = A_\zeta k_{\zeta *}\delta\left(k-k_{\zeta *}\right)\ ,\ \mathcal{P}_h = A_h k_{h*}\delta\left(k-k_{h*}\right)\ ,\ k_{\zeta *}=k_*\neq k_{h*}\ . \tag{34}$$

In Fig. 6, we plot the three kinds of power spectra $\mathcal{P}_a^{(2)}(a=1,2,3)$ in Eq. (28)–Eq. (30) for second order energy density perturbation $\delta^{(2)} = \delta\rho^{(2)}/\rho^{(0)}$ with different k_{h*}. As shown in Fig. 6, for $k_{h*} \neq k_{\zeta *}$, the behaviors of the power spectra $\mathcal{P}_2^{(2)}$ sourced by $\mathcal{S}_2 \sim \phi h$ are different from the case of $k_{h*}/k_{\zeta *} = 1$. More precisely, for $k_{h*}/k_{\zeta *} = n > 1$, the domain of definition of $\mathcal{P}_2^{(2)}$ is

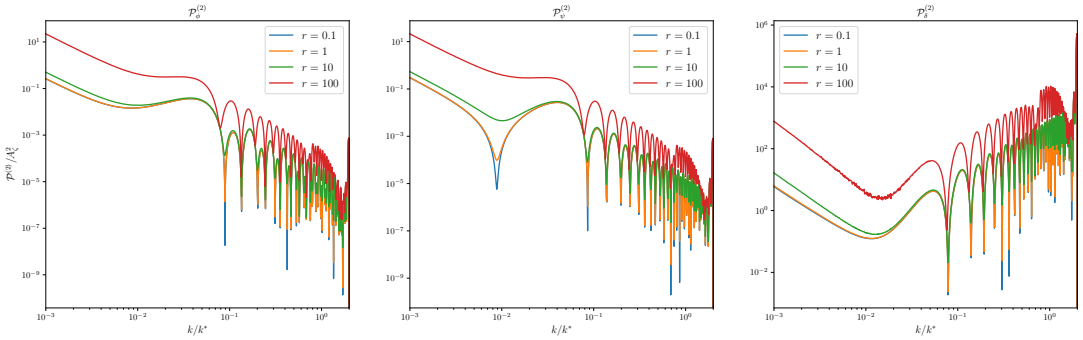


Fig. 5: The total power spectra of second order perturbations $\Phi^{(2)}$, $\Psi^{(2)}$, and $\delta^{(2)}$ for different tensor-to-scalar ratio $r = A_h/A_\zeta$. We have set $x_* = k_*\eta = 100$.

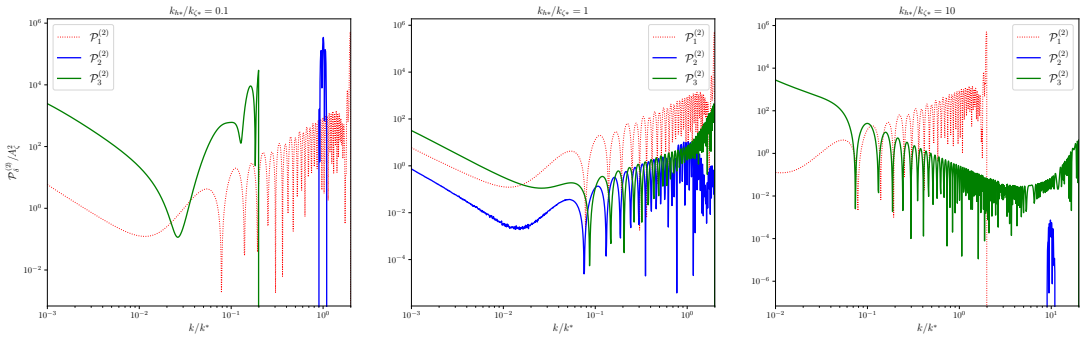


Fig. 6: The power spectra $\mathcal{P}_a^{(2)}(a = 1, 2, 3)$ for second order energy density perturbation $\delta^{(2)}$ with $k_{h*}/k_{\zeta*} = 0.1$, $k_{h*}/k_{\zeta*} = 1$, and $k_{h*}/k_{\zeta*} = 10$ respectively. We have set the tensor-to-scalar ratio $r = A_h/A_\zeta = 10$, $k_{\zeta*} = k_*$, and $x_* = k_*\eta = 100$.

$[(n-1)k/k_*, (n+1)k/k_*]$. For $k_{h*}/k_{\zeta*} = n \gg 1$, the power spectrum $\mathcal{P}_2^{(2)}$ becomes a small peak near $n \times k/k_*$. In this case, the contributions of the power spectra $\mathcal{P}_2^{(2)}$ can be neglected. And for $k_{h*}/k_{\zeta*} = n < 1$, the domain of definition of $\mathcal{P}_2^{(2)}$ is $[(1-n)k/k_*, (1+n)k/k_*]$. For $k_{h*}/k_{\zeta*} = n \ll 1$, the power spectra $\mathcal{P}_2^{(2)}$ sourced by $\mathcal{S}_2 \sim \phi h$ becomes a large peak near k/k_*.

As shown in Fig. 7, for $k_{h*}/k_{\zeta*} = 0.1$, the power spectra $\mathcal{P}_2^{(2)}$ can be larger than $\mathcal{P}_1^{(2)}$ sourced by $\mathcal{S}_1 \sim \phi\phi$ even in the case of $r = 0.1$. Note that the contributions of the source term $\mathcal{S}_2 \sim \phi h$ in Eq. (A.2) are completely neglected in previous studies [32, 35, 37]. Here, we point out that the contributions of the source term $\mathcal{S}_2 \sim \phi h$ are very important for the monochromatic primordial power spectra with $k_{h*}/k_{\zeta*} \ll 1$.

4 Log-normal primordial power spectra

Since the monochromatic primordial power spectra have infinitesimal width, it is necessary to consider a more realistic model, such as log-normal primordial power spectra. We consider the log-normal power spectra for primordial scalar and tensor perturbations. Here, we concentrated on

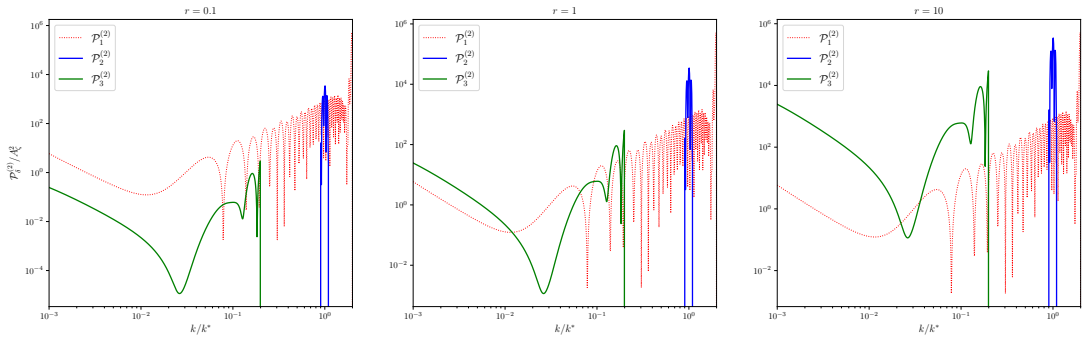


Fig. 7: The power spectra $\mathcal{P}_a^{(2)}(a=1,2,3)$ for second order energy density perturbation $\delta^{(2)}$ with $r=0.1$, $r=1$, and $r=10$ respectively. We have set $n=k_{h*}/k_{\zeta*}=0.1$, $k_{\zeta*}=k_*$, and $x_*=k_*\eta=100$.

the effects of the source term $\mathcal{S}_2\sim\phi h$ and corresponding second order power spectra $\mathcal{P}_2^{(2)}$. The log-normal primordial power spectra are given by

$$\mathcal{P}_\zeta=\frac{A_\zeta}{\sqrt{2\pi\sigma_*^2}}\exp\left(-\frac{\ln^2\left(\frac{k}{k_{\zeta*}}\right)}{2\sigma_*^2}\right)\,,\ \mathcal{P}_h=\frac{A_h}{\sqrt{2\pi\sigma_*^2}}\exp\left(-\frac{\ln^2\left(\frac{k}{k_{h*}}\right)}{2\sigma_*^2}\right)\,. \tag{35}$$

Here, we concentrate on the large peak of $\mathcal{P}_2^{(2)}$ with $k_{h*}/k_{\zeta*}\ll 1$. As mentioned in Sec. 3.2, for $k_{h*}/k_{\zeta*}=n\ll 1$, the power spectra $\mathcal{P}_2^{(2)}$ sourced by $\mathcal{S}_2\sim\phi h$ has a large peak near k/k_*. For the log-normal primordial power spectra, we calculate the power spectra of the second order density perturbation $\delta^{(2)}$ with $k_{h*}/k_{\zeta*}=0.1$. As shown in Fig. 8, for log-normal primordial power spectra, the peak of $\mathcal{P}_2^{(2)}$ becomes larger during the process of $\sigma_*\to 0$. For comparison, we plot $\mathcal{P}_1^{(2)}$ and $\mathcal{P}_2^{(2)}$ for the second order density perturbation $\delta^{(2)}$ with tensor-to-scalar ratio $r=0.1$ in Fig. 9. It shows that the contributions of $\mathcal{P}_2^{(2)}$ become smaller when σ_* increases. Namely, the effects of the source term $\mathcal{S}_2\sim\phi h$ become more obviously when σ_* and n become smaller.

5 Conclusions and discussions

In this paper, we systematically studied the second order density perturbations induced by primordial gravitational wave and primordial scalar perturbation. Since the constraints of primordial curvature and tensor perturbations on small scales are significantly weaker than those on large scales, we considered the large tensor-to-scalar ratio r on small scales. As shown in Fig. 5, the effects of the primordial tensor perturbation become obvious for $r\gg 1$. For tensor-to-scalar ratio $r\ll 1$, the effects of primordial tensor perturbation become negligible and our results of the power spectra $\mathcal{P}_\phi^{(2)}$, $\mathcal{P}_\psi^{(2)}$, and $\mathcal{P}_\delta^{(2)}$ reduce to the previous results in Ref. [32].

We give the explicit expressions for the power spectra of primordial scalar and tensor induced scalar and density perturbations in Eqs. (28)–(32). Specifically, for a given primordial scalar and tensor power spectra, the power spectra of the second order induced scalar and density perturbations can be calculated using these equations. In this paper, we considered the primordial power

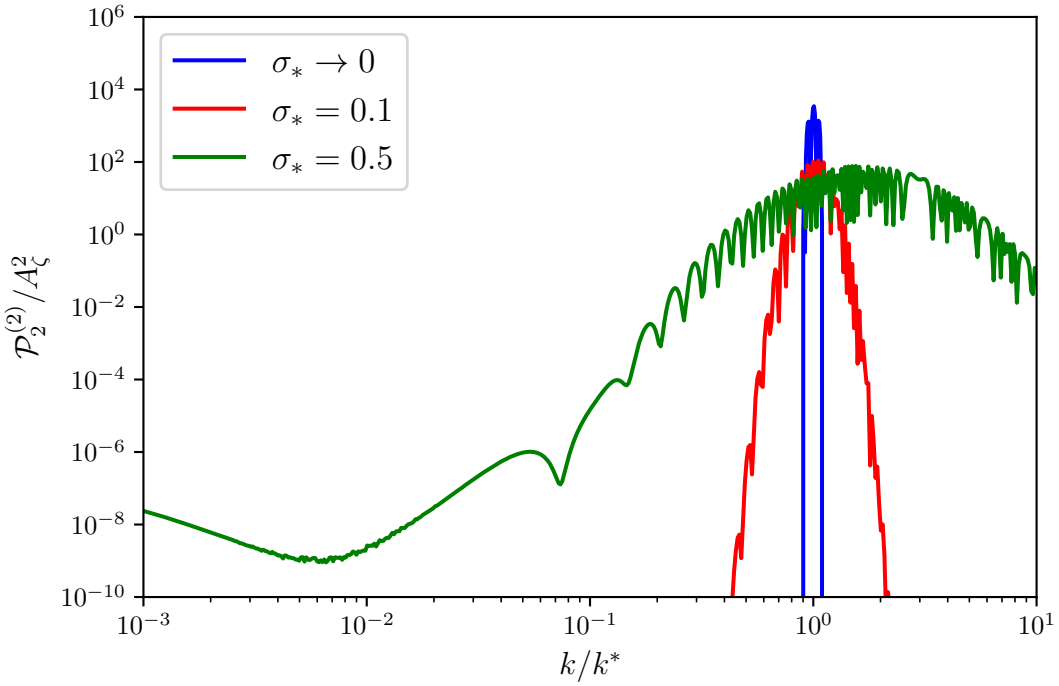


Fig. 8: The power spectra $\mathcal{P}_2^{(2)}$ sourced by $\mathcal{S}_2 \sim \phi h$ for second order energy density perturbation $\delta^{(2)}$ with $r = 0.1$. We have set $n = k_{h*}/k_{\zeta*} = 0.1$ and $x_* = k_*\eta = 100$.

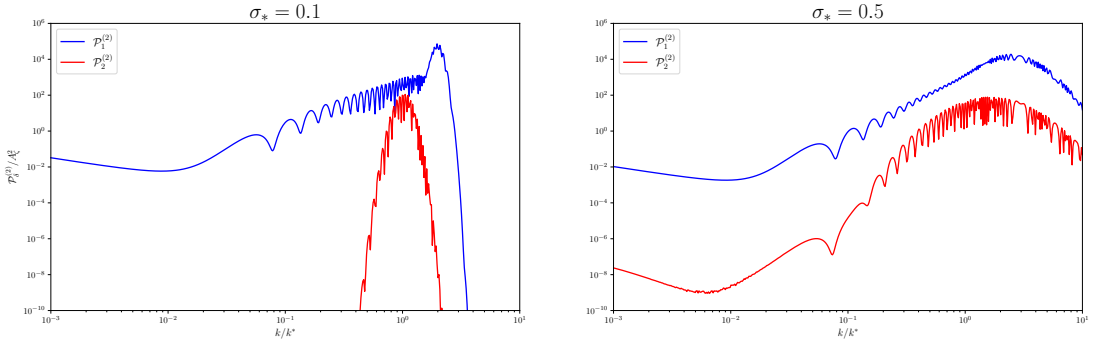


Fig. 9: The power spectra $\mathcal{P}_1^{(2)}$ and $\mathcal{P}_2^{(2)}$ for second order energy density perturbation $\delta^{(2)}$ with $r = 0.1$ for different σ_*. We have set $n = k_{h*}/k_{\zeta*} = 0.1$ and $x_* = k_*\eta = 100$.

spectra following delta and log-normal on small scales. It is essential to explore more general forms of the primordial power spectra, such as the log-normal primordial scalar power spectrum and the power-law primordial tensor power spectrum [67].

Moreover, the second order induced density perturbations offer a window to understand small-scale primordial gravitational waves and primordial curvature perturbations. More precisely, the primordial scalar and tensor power spectra can be calculated in terms of a given inflation model.

Using Eqs. (28)–(32), we can calculate the power spectra of second order induced scalar and energy density perturbations. The induced density perturbations will affect many physical processes at small scales, such as the formation of PBH [68] and the high order GW background [59]. By observing PBHs or higher order GWs, we can constrain the power spectrum of second order induced density perturbations, thereby constraining inflationary models and the physical properties of primordial scalar and gravitational wave on small scales. Related research might be given in future work.

Appendix A: Source terms

$$\begin{aligned}\mathcal{S}_{ij,1}\left(\mathbf{x},\eta\right)=&4\phi\partial_i\partial_j\phi+\partial_i\phi\partial_j\phi-\frac{\partial_i\phi'\partial_j\phi}{\mathcal{H}}-\frac{\partial_i\phi\partial_j\phi'}{\mathcal{H}}-\frac{\partial_i\phi'\partial_j\phi'}{\mathcal{H}^2}+\delta_{ij}\left(-24\mathcal{H}\phi\phi'\right.\\&\left.-2\left(\phi'\right)^2-4\phi\phi''-\frac{16}{3}\phi\Delta\phi-\frac{11}{3}\partial_b\phi\partial^b\phi+\frac{2}{3\mathcal{H}}\partial_b\phi'\partial^b\phi+\frac{1}{3\mathcal{H}^2}\partial_b\phi'\partial^b\phi'\right)\ ,\end{aligned}\tag{A.1}$$

$$\begin{aligned}\mathcal{S}_{ij,2}\left(\mathbf{x},\eta\right)=&-h_{ij}''\phi-2\mathcal{H}h_{ij}'\phi+10\mathcal{H}h_{ij}\phi'+3h_{ij}\phi''-\phi\Delta h_{ij}-\frac{5}{3}h_{ij}\Delta\phi+h_j^b\partial_b\partial_i\phi\\&+h_i^b\partial_b\partial_j\phi-2\partial_b h_{ij}\partial^b\phi+\partial^b\phi\partial_i h_{jb}+\partial^b\phi\partial_j h_{ib}-\delta_{ij}\frac{2}{3}h^{bc}\partial_c\partial_b\phi\ ,\end{aligned}\tag{A.2}$$

$$\begin{aligned}\mathcal{S}_{ij,3}\left(\mathbf{x},\eta\right)=&-\frac{1}{2}h_i^{b'}h_{jb}'+\frac{1}{2}h^{bc}\partial_c\partial_b h_{ij}-\frac{1}{2}h^{bc}\partial_c\partial_i h_{jb}-\frac{1}{2}h^{bc}\partial_c\partial_j h_{ib}-\frac{1}{2}\partial_b h_{jc}\partial^c h_i^b\\&+\frac{1}{2}\partial_c h_{jb}\partial^c h_i^b+\frac{1}{4}\partial_i h^{bc}\partial_j h_{bc}+\frac{1}{2}h^{bc}\partial_i\partial_j h_{bc}+\delta_{ij}\left(\frac{5}{12}h_{bc}'h'^{bc}+\frac{1}{2}h^{bc}h_{bc}''\right.\\&\left.+\frac{4\mathcal{H}}{3}h^{bc}h_{bc}'-\frac{2}{3}h^{bc}\Delta h_{bc}+\frac{1}{3}\partial_c h_{bd}\partial^d h^{bc}-\frac{1}{2}\partial_d h_{bc}\partial^d h^{bc}\right)\ ,\end{aligned}\tag{A.3}$$

where in Eqs. (A.1)–(A.3), we have defined $\partial_\eta\phi\equiv\phi'$. The source terms in momentum space are given by

$$\begin{aligned}S_{ij,1}\left(\mathbf{k},\eta\right)=&-\int\frac{d^3p}{(2\pi)^{3/2}}\left(4p_ip_jT_\phi(ux)T_\phi(vx)+((k-p)_ip_j)\left(T_\phi(ux)T_\phi(vx)-ux\frac{d}{d(ux)}T_\phi(ux)T_\phi(vx)\right.\right.\\&\left.-vxT_\phi(ux)\frac{d}{d(vx)}T_\phi(vx)-vux^2\frac{d}{d(ux)}T_\phi(ux)\frac{d}{d(vx)}T_\phi(vx)\right)-\delta_{ij}\left(-\frac{24vk^2}{x}T_\phi(ux)T_\phi'(vx)\right.\\&-2uvk^2T_\phi'(ux)T_\phi'(vx)-4v^2k^2T_\phi(ux)T_\phi''(vx)+\frac{16v^2k^2}{3}T_\phi(ux)T_\phi(vx)\\&+\frac{11k^2(1-u^2-v^2)}{6}T_\phi(ux)T_\phi(vx)-\frac{k^2(1-u^2-v^2)ux}{3}T_\phi'(ux)T_\phi(vx)\\&\left.\left.-\frac{k^2(1-u^2-v^2)x^2uv}{6}T_\phi'(ux)T_\phi'(vx)\right)\right)\frac{4}{9}\zeta_{\mathbf{k}-\mathbf{p}}\zeta_{\mathbf{p}}\ ,\end{aligned}\tag{A.4}$$

$$
\begin{aligned}
S_{ij,2}\left(\mathbf{k},\eta\right) = \int \frac{d^3p}{(2\pi)^{3/2}} \Big(& -\left((k-p)^b p_i\right) \varepsilon^{\lambda}_{jb}\left(\mathbf{p}\right) T_\phi(ux) T_h(vx) - \left((k-p)^b p_j\right) \varepsilon^{\lambda}_{ib}\left(\mathbf{p}\right) T_\phi(ux) T_h(vx) \\
& - \left((k-p)_b (k-p)_i\right) \varepsilon^{\lambda,b}_{j}\left(\mathbf{p}\right) T_\phi(ux) T_h(vx) - \left((k-p)_b (k-p)_j\right) \varepsilon^{\lambda,b}_{i}\left(\mathbf{p}\right) T_\phi(ux) T_h(vx) \\
& + \varepsilon^{\lambda}_{ij}\left(\mathbf{p}\right) \Bigg(-v^2 k^2 T_\phi(ux) \frac{d^2}{d(vx)^2} T_h(vx) - \frac{2vk^2}{x} T_\phi(ux) \frac{d}{d(vx)} T_h(vx) \\
& + 3u^2 k^2 \frac{d^2}{d(ux)^2} T_\phi(ux) T_h(vx) + v^2 k^2 T_\phi(ux) T_h(vx) + \frac{5u^2 k^2}{3} T_\phi(ux) T_h(vx) \\
& + k^2 \left(1 - v^2 - u^2\right) T_\phi(ux) T_h(vx) + \frac{10uk^2}{x} \frac{d}{d(ux)} T_\phi(ux) T_h(vx) \Bigg) \\
& + \delta_{ij} \varepsilon^{\lambda,bc}(\mathbf{p}) (k-p)_b (k-p)_c \left(\frac{2}{3} T_\phi(ux) T_h(vx) \right) \Big) \frac{2}{3} \zeta_{\mathbf{k}-\mathbf{p}} \mathbf{h}^{\lambda}_{\mathbf{p}} \ ,
\end{aligned}
\tag{A.5}
$$

$$
\begin{aligned}
S_{ij,3}\left(\mathbf{k},\eta\right) = \int \frac{d^3p}{(2\pi)^{3/2}} \frac{1}{2} \Bigg(& \varepsilon^{\lambda_1,b}_{i}\left(\mathbf{k}-\mathbf{p}\right) \varepsilon^{\lambda_2}_{jb}\left(\mathbf{p}\right) \Bigg(-uvk^2 \frac{d}{(ux)} T_h(ux) \frac{d}{(vx)} T_h(vx) \\
& - \frac{k^2(1-v^2-u^2)}{2} T_h(ux) T_h(vx) \Bigg) - \varepsilon^{\lambda_1,bc}(\mathbf{k}-\mathbf{p}) \varepsilon^{\lambda_2}_{ij}(\mathbf{p}) p_b p_c T_h(ux) T_h(vx) \\
& + \varepsilon^{\lambda_1,bc}(\mathbf{k}-\mathbf{p}) \varepsilon^{\lambda_2}_{jb}(\mathbf{p}) p_c p_i T_h(ux) T_h(vx) + \varepsilon^{\lambda_1,bc}(\mathbf{k}-\mathbf{p}) \varepsilon^{\lambda_2}_{ib}(\mathbf{p}) p_c p_j T_h(ux) T_h(vx) \\
& - \varepsilon^{\lambda_1,bc}(\mathbf{k}-\mathbf{p}) \varepsilon^{\lambda_2}_{bc}(\mathbf{p}) \left(\frac{1}{2} (k-p)_i p_j T_h(ux) T_h(vx) + p_i p_j T_h(ux) T_h(vx) \right) \\
& + \varepsilon^{\lambda_1}_{jc}(\mathbf{k}-\mathbf{p}) \varepsilon^{\lambda_2,b}_{i}(\mathbf{p}) (k-p)_b p^c T_h(ux) T_h(vx) \\
& + 2\delta_{ij} \Bigg(\varepsilon^{\lambda_1}_{bc}(\mathbf{k}-\mathbf{p}) \varepsilon^{\lambda_2,bc}(\mathbf{p}) \Bigg(\frac{5uvk^2}{12} T'_h(ux) T'_h(vx) + \frac{v^2k^2}{2} T_h(ux) T''_h(vx) \\
& + \frac{4vk^2}{3x} T_h(ux) T'_h(vx) + \frac{2v^2k^2}{3} T_h(ux) T_h(vx) + \frac{k^2(1-u^2-v^2)}{4} T_h(ux) T_h(vx) \Bigg) \\
& - \frac{1}{3} \varepsilon^{\lambda_1}_{bd}(\mathbf{k}-\mathbf{p}) \varepsilon^{\lambda_2,bc}(\mathbf{p}) (k-p)_c p^d T_h(ux) T_h(vx) \Bigg) \Bigg) \mathbf{h}^{\lambda_1}_{\mathbf{k}-\mathbf{p}} \mathbf{h}^{\lambda_2}_{\mathbf{p}} \ .
\end{aligned}
\tag{A.6}
$$

In Eqs. (A.4)–(A.6), we have defined $|\mathbf{k}-\mathbf{p}| = u|\mathbf{k}| = uk$ and $p = |\mathbf{p}| = vk$.The explicit expressions of the polarization tensor $\varepsilon^{\lambda_1,ij}(\mathbf{p})$ are given in Appendix B. The first order scalar and tensor perturbations in Eqs. (A.4)–(A.6) have been written as

$$
\psi(\eta,\mathbf{k}) = \phi(\eta,\mathbf{k}) = \frac{2}{3} \zeta_{\mathbf{k}} T_\phi(k\eta) \ , \ h^{\lambda}(\eta,\mathbf{k}) = \mathbf{h}^{\lambda}_{\mathbf{k}} T_h(k\eta) \ , \tag{A.7}
$$

where $\zeta_{\mathbf{k}}$ and $\mathbf{h}_{\mathbf{k}}$ are the primordial curvature and tensor perturbations respectively. The transfer functions $T_\phi(k\eta)$ and $T_h(k\eta)$ in the RD era are given by [32]

$$
T_\phi(x) = \frac{9}{x^2} \left(\frac{\sqrt{3}}{x} \sin\left(\frac{x}{\sqrt{3}}\right) - \cos\left(\frac{x}{\sqrt{3}}\right) \right) \ , \ T_h = \frac{\sin x}{x} \ . \tag{A.8}
$$

Appendix B: Polarization tensor

The polarization tensor is defined as

$$
\varepsilon^{\times}_{ij}\left(\mathbf{k}\right) = \frac{1}{\sqrt{2}} \left(e_i\left(\mathbf{k}\right) \bar{e}_j\left(\mathbf{k}\right) + \bar{e}_i\left(\mathbf{k}\right) e_j\left(\mathbf{k}\right) \right) \ , \tag{B.9}
$$

$$\varepsilon_{ij}^{+}\left(\mathbf{k}\right)=\frac{1}{\sqrt{2}}\left(e_i\left(\mathbf{k}\right)e_j\left(\mathbf{k}\right)-\bar{e}_i\left(\mathbf{k}\right)\bar{e}_j\left(\mathbf{k}\right)\right)\ , \tag{B.10}$$

where $\left(\mathbf{k}_i/|k|, e_i\left(\mathbf{k}\right), \bar{e}_i\left(\mathbf{k}\right)\right)$ is the normalized bases in three dimensional momentum space. We study the polarization tensor for a given coordinate system, namely

$$\mathbf{k}=(0,0,k)\ ,\ e_i\left(\mathbf{k}\right)=(1,0,0)\ ,\ \bar{e}_i\left(\mathbf{k}\right)=(0,1,0)\ . \tag{B.11}$$

Then the polarization tensors $\varepsilon_{ij}^{\lambda}\left(\mathbf{k}-\mathbf{p}\right)$ and $\varepsilon_{ij}^{\lambda}\left(\mathbf{p}\right)$ can be written as

$$\begin{aligned}
\varepsilon_{ij}^{\times}\left(\mathbf{k}-\mathbf{p}\right)&=\frac{1}{\sqrt{2}}\left(e_i\left(\mathbf{k}-\mathbf{p}\right)\bar{e}_j\left(\mathbf{k}-\mathbf{p}\right)+\bar{e}_i\left(\mathbf{k}-\mathbf{p}\right)e_j\left(\mathbf{k}-\mathbf{p}\right)\right)\ ,\\
\varepsilon_{ij}^{+}\left(\mathbf{k}-\mathbf{p}\right)&=\frac{1}{\sqrt{2}}\left(e_i\left(\mathbf{k}-\mathbf{p}\right)e_j\left(\mathbf{k}-\mathbf{p}\right)-\bar{e}_i\left(\mathbf{k}-\mathbf{p}\right)\bar{e}_j\left(\mathbf{k}-\mathbf{p}\right)\right)\ ,\\
\varepsilon_{ij}^{\times}\left(\mathbf{p}\right)&=\frac{1}{\sqrt{2}}\left(e_i\left(\mathbf{p}\right)\bar{e}_j\left(\mathbf{p}\right)+\bar{e}_i\left(\mathbf{p}\right)e_j\left(\mathbf{p}\right)\right)\ ,\\
\varepsilon_{ij}^{+}\left(\mathbf{p}\right)&=\frac{1}{\sqrt{2}}\left(e_i\left(\mathbf{p}\right)e_j\left(\mathbf{p}\right)-\bar{e}_i\left(\mathbf{p}\right)\bar{e}_j\left(\mathbf{p}\right)\right)\ ,
\end{aligned} \tag{B.12}$$

where

$$\begin{aligned}
\mathbf{k}-\mathbf{p}&=k\left(-\sqrt{v^2-\frac{1}{4}\left(-u^2+v^2+1\right)^2},0,\frac{1}{2}\left(u^2-v^2+1\right)\right)\ ,\\
e_i\left(\mathbf{k}-\mathbf{p}\right)&=\left(\frac{u^2-v^2+1}{2u},0,\frac{\sqrt{-u^4+2u^2v^2+2u^2-v^4+2v^2-1}}{2u}\right)\ ,\\
\bar{e}_i\left(\mathbf{k}-\mathbf{p}\right)&=(0,1,0)\ ,
\end{aligned} \tag{B.13}$$

$$\begin{aligned}
\mathbf{p}&=k\left(\sqrt{v^2-\frac{1}{4}\left(-u^2+v^2+1\right)^2},0,\frac{1}{2}\left(-u^2+v^2+1\right)\right)\ ,\\
e_i\left(\mathbf{p}\right)&=\left(-\frac{-u^2+v^2+1}{2v},0,\frac{\sqrt{-u^4+2u^2\left(v^2+1\right)-\left(v^2-1\right)^2}}{2v}\right)\ ,\\
\bar{e}_i\left(\mathbf{p}\right)&=(0,1,0)\ .
\end{aligned} \tag{B.14}$$

Appendix C: four-point function

$$\begin{aligned}
\left\langle\zeta_{\mathbf{k}-\mathbf{p}}\zeta_{\mathbf{p}}\zeta_{\mathbf{k}'-\mathbf{p}'}\zeta_{\mathbf{p}'}\right\rangle&=\left\langle\zeta_{\mathbf{k}-\mathbf{p}}\zeta_{\mathbf{k}'-\mathbf{p}'}\right\rangle\left\langle\zeta_{\mathbf{p}}\zeta_{\mathbf{p}'}\right\rangle+\left\langle\zeta_{\mathbf{k}-\mathbf{p}}\zeta_{\mathbf{p}'}\right\rangle\left\langle\zeta_{\mathbf{p}}\zeta_{\mathbf{k}'-\mathbf{p}'}\right\rangle\\
&=\delta\left(\mathbf{k}+\mathbf{k}'\right)\frac{(2\pi^2)^2}{p^3|\mathbf{k}-\mathbf{p}|^3}\left(\delta\left(\mathbf{p}+\mathbf{p}'\right)+\delta\left(\mathbf{k}'-\mathbf{p}'+\mathbf{p}\right)\right)\mathcal{P}_\zeta(|\mathbf{k}-\mathbf{p}|)\mathcal{P}_\zeta(p)\ ,
\end{aligned} \tag{C.15}$$

$$\begin{aligned}
\langle\zeta_{\mathbf{k}-\mathbf{p}}\mathbf{h}_{\mathbf{p}}^{\lambda_1}\zeta_{\mathbf{k}'-\mathbf{p}'}\mathbf{h}_{\mathbf{p}'}^{\lambda_1'}\rangle=&\langle\zeta_{\mathbf{k}-\mathbf{p}}\zeta_{\mathbf{k}'-\mathbf{p}'}\rangle\langle\mathbf{h}_{\mathbf{p}}^{\lambda_1}\mathbf{h}_{\mathbf{p}'}^{\lambda_1'}\rangle\\
=&\delta\left(\mathbf{k}+\mathbf{k}'\right)\delta^{\lambda_1\lambda_1'}\frac{(2\pi^2)^2}{p^3|\mathbf{k}-\mathbf{p}|^3}\delta\left(\mathbf{p}+\mathbf{p}'\right)\mathcal{P}_\zeta(|\mathbf{k}-\mathbf{p}|)\mathcal{P}_h(p)\ ,
\end{aligned} \tag{C.16}$$

$$\begin{aligned}
\langle\mathbf{h}_{\mathbf{k}-\mathbf{p}}^{\lambda_1}\mathbf{h}_{\mathbf{p}}^{\lambda_2}\mathbf{h}_{\mathbf{k}'-\mathbf{p}'}^{\lambda_1'}\mathbf{h}_{\mathbf{p}'}^{\lambda_2'}\rangle=&\delta\left(\mathbf{k}+\mathbf{k}'\right)\frac{(2\pi^2)^2}{p^3|\mathbf{k}-\mathbf{p}|^3}\left(\delta^{\lambda_1\lambda_1'}\delta^{\lambda_2\lambda_2'}\delta\left(\mathbf{p}+\mathbf{p}'\right)+\delta^{\lambda_1\lambda_2'}\delta^{\lambda_2\lambda_1'}\delta\left(\mathbf{k}'-\mathbf{p}'+\mathbf{p}\right)\right)\\
&\times\mathcal{P}_h(|\mathbf{k}-\mathbf{p}|)\mathcal{P}_h(p)\ .
\end{aligned} \tag{C.17}$$

References

1. N. Aghanim et al. Planck 2018 results. VI. Cosmological parameters. *Astron. Astrophys.*, 641:A6, 2020. [Erratum: Astron.Astrophys. 652, C4 (2021)].
2. Karim A. Malik and David Wands. Cosmological perturbations. *Phys. Rept.*, 475:1–51, 2009.
3. Viatcheslav F. Mukhanov, H. A. Feldman, and Robert H. Brandenberger. Theory of cosmological perturbations. Part 1. Classical perturbations. Part 2. Quantum theory of perturbations. Part 3. Extensions. *Phys. Rept.*, 215:203–333, 1992.
4. Hideo Kodama and Misao Sasaki. Cosmological Perturbation Theory. *Prog. Theor. Phys. Suppl.*, 78:1–166, 1984.
5. Silvia Mollerach, Diego Harari, and Sabino Matarrese. CMB polarization from secondary vector and tensor modes. *Phys. Rev. D*, 69:063002, 2004.
6. Daniel Baumann, Paul J. Steinhardt, Keitaro Takahashi, and Kiyotomo Ichiki. Gravitational Wave Spectrum Induced by Primordial Scalar Perturbations. *Phys. Rev. D*, 76:084019, 2007.
7. Kazunori Kohri and Takahiro Terada. Semianalytic calculation of gravitational wave spectrum nonlinearly induced from primordial curvature perturbations. *Phys. Rev. D*, 97(12):123532, 2018.
8. Guillem Domènech. Scalar Induced Gravitational Waves Review. *Universe*, 7(11):398, 2021.
9. Zhe Chang, Xukun Zhang, and Jing-Zhi Zhou. Primordial black holes and third order scalar induced gravitational waves. 9 2022.
10. Alba Romero-Rodriguez, Mario Martinez, Oriol Pujolàs, Mairi Sakellariadou, and Ville Vaskonen. Search for a Scalar Induced Stochastic Gravitational Wave Background in the Third LIGO-Virgo Observing Run. *Phys. Rev. Lett.*, 128(5):051301, 2022.
11. Ryo Saito and Jun'ichi Yokoyama. Gravitational wave background as a probe of the primordial black hole abundance. *Phys. Rev. Lett.*, 102:161101, 2009. [Erratum: Phys.Rev.Lett. 107, 069901 (2011)].
12. Sai Wang, Takahiro Terada, and Kazunori Kohri. Prospective constraints on the primordial black hole abundance from the stochastic gravitational-wave backgrounds produced by coalescing events and curvature perturbations. *Phys. Rev. D*, 99(10):103531, 2019. [Erratum: Phys.Rev.D 101, 069901 (2020)].
13. Keisuke Inomata and Tomohiro Nakama. Gravitational waves induced by scalar perturbations as probes of the small-scale primordial spectrum. *Phys. Rev. D*, 99(4):043511, 2019.
14. Enrico Barausse et al. Prospects for Fundamental Physics with LISA. *Gen. Rel. Grav.*, 52(8):81, 2020.
15. N. Bartolo, V. De Luca, G. Franciolini, A. Lewis, M. Peloso, and A. Riotto. Primordial Black Hole Dark Matter: LISA Serendipity. *Phys. Rev. Lett.*, 122(21):211301, 2019.
16. Rong-gen Cai, Shi Pi, and Misao Sasaki. Gravitational Waves Induced by non-Gaussian Scalar Perturbations. *Phys. Rev. Lett.*, 122(20):201101, 2019.
17. Zhe Chang, Xukun Zhang, and Jing-Zhi Zhou. Gravitational waves from primordial scalar and tensor perturbations. *Phys. Rev. D*, 107(6):063510, 2023.
18. Keisuke Inomata, Masahiro Kawasaki, Kyohei Mukaida, Yuichiro Tada, and Tsutomu T. Yanagida. Inflationary primordial black holes for the LIGO gravitational wave events and pulsar timing array experiments. *Phys. Rev. D*, 95(12):123510, 2017.

19. Theodoros Papanikolaou, Vincent Vennin, and David Langlois. Gravitational waves from a universe filled with primordial black holes. *JCAP*, 03:053, 2021.
20. Zihan Zhou, Jie Jiang, Yi-Fu Cai, Misao Sasaki, and Shi Pi. Primordial black holes and gravitational waves from resonant amplification during inflation. *Phys. Rev. D*, 102(10):103527, 2020.
21. Guillem Domènech, Shi Pi, and Misao Sasaki. Induced gravitational waves as a probe of thermal history of the universe. *JCAP*, 08:017, 2020.
22. Rong-Gen Cai, Zong-Kuan Guo, Jing Liu, Lang Liu, and Xing-Yu Yang. Primordial black holes and gravitational waves from parametric amplification of curvature perturbations. *JCAP*, 06:013, 2020.
23. Rong-Gen Cai, Shi Pi, Shao-Jiang Wang, and Xing-Yu Yang. Pulsar Timing Array Constraints on the Induced Gravitational Waves. *JCAP*, 10:059, 2019.
24. Chen Yuan, Zu-Cheng Chen, and Qing-Guo Huang. Probing primordial–black-hole dark matter with scalar induced gravitational waves. *Phys. Rev. D*, 100(8):081301, 2019.
25. Nicola Bartolo, Valerie Domcke, Daniel G. Figueroa, Juan García-Bellido, Marco Peloso, Mauro Pieroni, Angelo Ricciardone, Mairi Sakellariadou, Lorenzo Sorbo, and Gianmassimo Tasinato. Probing non-Gaussian Stochastic Gravitational Wave Backgrounds with LISA. *JCAP*, 11:034, 2018.
26. Laila Alabidi, Kazunori Kohri, Misao Sasaki, and Yuuiti Sendouda. Observable induced gravitational waves from an early matter phase. *JCAP*, 05:033, 2013.
27. Xukun Zhang, Jing-Zhi Zhou, and Zhe Chang. Impact of the free-streaming neutrinos to the second order induced gravitational waves. *Eur. Phys. J. C*, 82(9):781, 2022.
28. Jinn-Ouk Gong. Analytic Integral Solutions for Induced Gravitational Waves. *Astrophys. J.*, 925(1):102, 2022.
29. Jing-Zhi Zhou, Xukun Zhang, Qing-Hua Zhu, and Zhe Chang. The third order scalar induced gravitational waves. *JCAP*, 05(05):013, 2022.
30. K. G. Arun et al. New horizons for fundamental physics with LISA. *Living Rev. Rel.*, 25(1):4, 2022.
31. Zhi-Chao Zhao and Sai Wang. Bayesian implications for the primordial black holes from NANOGrav's pulsar-timing data by using the scalar induced gravitational waves. 11 2022.
32. Keisuke Inomata. Analytic solutions of scalar perturbations induced by scalar perturbations. *JCAP*, 03:013, 2021.
33. Pedro Carrilho and Karim A. Malik. Vector and tensor contributions to the curvature perturbation at second order. *JCAP*, 02:021, 2016.
34. Yang Zhang, Fei Qin, and Bo Wang. Second-order cosmological perturbations. II. Produced by scalar-tensor and tensor-tensor couplings. *Phys. Rev. D*, 96(10):103523, 2017.
35. Tomohiro Nakama and Teruaki Suyama. Primordial black holes as a novel probe of primordial gravitational waves. II: Detailed analysis. *Phys. Rev. D*, 94(4):043507, 2016.
36. Tomohiro Nakama and Teruaki Suyama. Primordial black holes as a novel probe of primordial gravitational waves. *Phys. Rev. D*, 92(12):121304, 2015.
37. Pritha Bari, Angelo Ricciardone, Nicola Bartolo, Daniele Bertacca, and Sabino Matarrese. Signatures of Primordial Gravitational Waves on the Large-Scale Structure of the Universe. *Phys. Rev. Lett.*, 129(9):091301, 2022.

38. Inyong Cho, Jinn-Ouk Gong, and Seung Hun Oh. Second-order effective energy-momentum tensor of gravitational scalar perturbations with perfect fluid. *Phys. Rev. D*, 102(4):043531, 2020.
39. Shohei Saga. *The Vector Mode in the Second-order Cosmological Perturbation Theory*. PhD thesis, Nagoya U. (main), 2017.
40. Teresa Hui-Ching Lu, Kishore Ananda, and Chris Clarkson. Vector modes generated by primordial density fluctuations. *Phys. Rev. D*, 77:043523, 2008.
41. Teresa Hui-Ching Lu, Kishore Ananda, Christopher Clarkson, and Roy Maartens. The cosmological background of vector modes. *JCAP*, 02:023, 2009.
42. Robert E. Smith, Ravi K. Sheth, and Roman Scoccimarro. An analytic model for the bispectrum of galaxies in redshift space. *Phys. Rev. D*, 78:023523, 2008.
43. Viviana Acquaviva, Nicola Bartolo, Sabino Matarrese, and Antonio Riotto. Second order cosmological perturbations from inflation. *Nucl. Phys. B*, 667:119–148, 2003.
44. Marc Kamionkowski, Arthur Kosowsky, and Albert Stebbins. A Probe of primordial gravity waves and vorticity. *Phys. Rev. Lett.*, 78:2058–2061, 1997.
45. Ruth Durrer. Light deflection in perturbed Friedmann universes. *Phys. Rev. Lett.*, 72:3301–3304, 1994.
46. Daisuke Yamauchi, Toshiya Namikawa, and Atsushi Taruya. Weak lensing generated by vector perturbations and detectability of cosmic strings. *JCAP*, 10:030, 2012.
47. Shohei Saga, Daisuke Yamauchi, and Kiyotomo Ichiki. Weak lensing induced by second-order vector mode. *Phys. Rev. D*, 92(6):063533, 2015.
48. Zhe Chang, Xukun Zhang, and Jing-Zhi Zhou. The cosmological vector modes from a monochromatic primordial power spectrum. *JCAP*, 10:084, 2022.
49. Y. Akrami et al. Planck 2018 results. X. Constraints on inflation. *Astron. Astrophys.*, 641:A10, 2020.
50. Torsten Bringmann, Pat Scott, and Yashar Akrami. Improved constraints on the primordial power spectrum at small scales from ultracompact minihalos. *Phys. Rev. D*, 85:125027, 2012.
51. Kishore N. Ananda, Chris Clarkson, and David Wands. The Cosmological gravitational wave background from primordial density perturbations. *Phys. Rev. D*, 75:123518, 2007.
52. Laila Alabidi, Kazunori Kohri, Misao Sasaki, and Yuuiti Sendouda. Observable Spectra of Induced Gravitational Waves from Inflation. *JCAP*, 09:017, 2012.
53. Edgar Bugaev and Peter Klimai. Induced gravitational wave background and primordial black holes. *Phys. Rev. D*, 81:023517, 2010.
54. Keisuke Inomata, Masahiro Kawasaki, Kyohei Mukaida, and Tsutomu T. Yanagida. Double inflation as a single origin of primordial black holes for all dark matter and LIGO observations. *Phys. Rev. D*, 97(4):043514, 2018.
55. Juan Garcia-Bellido, Marco Peloso, and Caner Unal. Gravitational Wave signatures of inflationary models from Primordial Black Hole Dark Matter. *JCAP*, 09:013, 2017.
56. Misao Sasaki, Teruaki Suyama, Takahiro Tanaka, and Shuichiro Yokoyama. Primordial black holes—perspectives in gravitational wave astronomy. *Class. Quant. Grav.*, 35(6):063001, 2018.
57. Tsutomu Kobayashi, Masahide Yamaguchi, and Jun'ichi Yokoyama. Generalized G-inflation: Inflation with the most general second-order field equations. *Prog. Theor. Phys.*, 126:511–529, 2011.

58. Mohammad Ali Gorji and Misao Sasaki. Primordial-tensor-induced stochastic gravitational waves. *Phys. Lett. B*, 846:138236, 2023.
59. Chao Chen, Atsuhisa Ota, Hui-Yu Zhu, and Yuhang Zhu. Missing one-loop contributions in secondary gravitational waves. 10 2022.
60. Pritha Bari, Nicola Bartolo, Guillem Domènech, and Sabino Matarrese. Gravitational waves induced by scalar-tensor mixing. 7 2023.
61. Raphael Picard and Karim A. Malik. Induced gravitational waves: the effect of first order tensor perturbations. 11 2023.
62. Inyong Cho, Jinn-Ouk Gong, and Seung Hun Oh. Second-order energy-momentum tensor of a scalar field. *Phys. Rev. D*, 106(8):084027, 2022.
63. Cyril Pitrou, Xavier Roy, and Obinna Umeh. xPand: An algorithm for perturbing homogeneous cosmologies. *Class. Quant. Grav.*, 30:165002, 2013.
64. N. Bartolo, E. Komatsu, Sabino Matarrese, and A. Riotto. Non-Gaussianity from inflation: Theory and observations. *Phys. Rept.*, 402:103–266, 2004.
65. Nicola Bartolo, Sabino Matarrese, and Antonio Riotto. Gauge-invariant temperature anisotropies and primordial non-Gaussianity. *Phys. Rev. Lett.*, 93:231301, 2004.
66. Sam Young and Christian T. Byrnes. Signatures of non-gaussianity in the isocurvature modes of primordial black hole dark matter. *JCAP*, 04:034, 2015.
67. Yan-Heng Yu and Sai Wang. Primordial Gravitational Waves Assisted by Cosmological Scalar Perturbations. 3 2023.
68. Valerio De Luca, Alex Kehagias, and Antonio Riotto. How well do we know the primordial black hole abundance: The crucial role of nonlinearities when approaching the horizon. *Phys. Rev. D*, 108(6):063531, 2023.